2020 IEEE International Conference on Robotics and Automation (ICRA)
31 May - 31 August, 2020. Paris, France

Acoustofluidic Tweezers for the 3D Manipulation of Microparticles*

Xinyi Guo, Zhichao Ma, Rahul Goyal, Moonkwang Jeong, Wei Pang, Peer Fischer, Xuexin Duan and Tian Qiu

Abstract— **Non-contact manipulation is of great importance in the actuation of micro-robotics. It is challenging to contactless manipulate micro-scale objects over large spatial distance in fluid. Here, we describe a novel approach for the dynamic position control of microparticles in three-dimensional (3D) space, based on high-speed acoustic streaming generated by a micro-fabricated gigahertz transducer. The hydrodynamic force generated by the streaming flow field has a vertical component against gravity and a lateral component towards the center, thus the microparticle is able to be stably trapped at a position far from the transducer surface, and to be manipulated over centimeter distance in 3D. Only the hydrodynamic force is utilized in the system for particle manipulation, making it a versatile tool regardless the material properties of the trapped particle. The system shows high reliability and manipulation velocity, revealing its potentials for the applications in robotics and automation at small scales.**

I. INTRODUCTION

The manipulation of micro-objects is of great interest in robotics and automation at small scales. Traditional manipulation methods often require direct contact and can thus be limited at this scale. Solid contacts can easily induce deformation or damage soft or biological materials, and the dominance of surface forces over volume forces makes it difficult to precisely manipulate and especially to release micro-objects [1]. To overcome these obstacles, numerous contactless manipulation approaches have been developed, such as magnetic tweezers [2], dielectrophoresis [3] and optical tweezers [4-6]. These methods have been used for various applications in biology and physics, such as microparticle or cell trapping and transportation [2, 7], molecular force measurements [8], and three-dimensional (3D) assembly [9, 10]. However, these strategies require special material properties of the manipulated object. For example, magnetic tweezers require magnetic materials, dielectrophoresis depend on the difference in dielectric properties between the particle and the medium.

* This work was supported by the Max Planck Society and the European Research Council under the ERC Grant agreement HOLOMAN (788296).

X. Guo, Z. Ma, R. Goyal, M. Jeong, P. Fischer and T. Qiu are with Max Planck Institute for Intelligent Systems, 70569 Stuttgart, Germany.

X. Guo, W. Pang and X. Duan are with the State Key Laboratory of Precision Measuring Technology & Instruments, Tianjin University, Tianjin 300072, China.

X. Guo, W. Pang and X. Duan are also with the College of Precision Instrument and Opto-electronics Engineering, Tianjin University, Tianjin 300072, China.

P. Fischer and T. Qiu are also with the Institute of Physical Chemistry, University of Stuttgart, Pfaffenwaldring 55, 70569 Stuttgart, Germany. (corresponding author: T. Qiu; +49 711 685 64482; e-mail: tian.qiu@ipc.uni-stuttgart.de).

Acoustic tweezers use acoustic radiation forces to manipulate particles without contact and work with a large range of materials in various media [11]. Using standing waves, particles can be trapped at fixed positions [12, 13], and transportation in one [14] or multiple [15-17] dimensions is enabled by changing phase [18], driving frequency [19] or acoustic streaming [20]. Most of these approaches were restricted to small microfluidic chambers with confined geometries or very close to the surface of the ultrasonic transducer [21]. We recently developed the acoustic hologram technology, and demonstrated that with the phase modulation of a travelling plane wave can generate a complicated 3D acoustic field and achieve the particle manipulation in an arbitrary trajectory [22]. Nevertheless, it is difficult to form a stable 3D trap with the travelling wave, as the particle is pushed away in the travelling direction of the wave, and the trapping force is also dependent on the acoustic contrast between the particle and the medium.

Hydrodynamic tweezers offer a unique chance to trap microparticles in fluids in a contactless manner with no restrictions on the materials properties. It has been shown that steady streaming vortices can be generated around an obstruction [23] or a cavity [24-26], or on the edge of an acoustic field [27] in a microfluidic channel, and trap particles in the center of the eddies. We showed that the excitation of bubble resonances can be used to realize a wireless robot arm at a distance [28, 29], but it requires a transducer area of ~10 mm^2. Researchers also demonstrated that the magnetically actuated rotation of beads [30, 31] or dumbbell structures [32] can form micro-vortices to trap and manipulate microspheres and motile microorganisms. However, hydrodynamic tweezers based on the vortices only work in a very close distance to the solid boundaries, which limits their application in the long-range distance in the 3D space.

Here, we demonstrate a novel and simple contactless microparticle manipulation method based on the acoustic streaming generated by a micro-fabricated gigahertz transducer (Fig. 1). In contrast to kHz and MHz frequencies, which have been used for acoustic manipulation, gigahertz sound waves attenuate strongly in liquid, leading to a high-speed jet flow perpendicular to the resonant surface for the particle levitation. The vertical position of the particle can be controlled by acoustic power and occurs when the upward force and the gravitational pull on the particle balance. Its horizontal trapping position is induced by the pressure difference generated by the oblique fluid motion on the two sides of the particle. A stable trap for an individual microparticle is formed in the bulk fluid and far away from the transducer surface. We show that the controlled manipulation of the microparticle can be achieved with the new method over centimeter distance in all three spatial directions.

978-1-7281-7395-5/20/$31.00 ©2020 IEEE

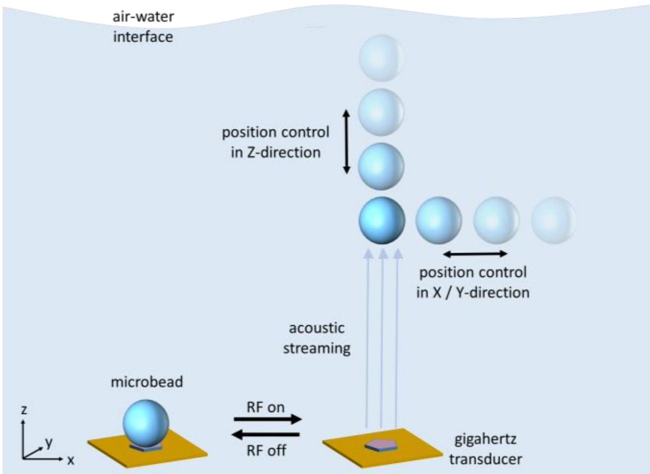

Figure 1. Schematic of the acoustofluidic tweezers for the microparticle manipulation. The stable 3D trap is generated in water with the acoustic streaming induced by the gigahertz ultrasonic transducer.

II. MATERIALS AND METHODS

A. Gigahertz ultrasonic transducer

The gigahertz ultrasonic transducer was designed and fabricated based on MEMS technology. Briefly, a Bragg reflector composed of alternating layers of silicon dioxide (SiO_2) and molybdenum (Mo) (SiO_2 / Mo / SiO_2 / Mo / SiO_2, 650 / 640 / 650 / 640 / 650 nm thick each) was firstly deposited on a Si substrate (400 µm thick) to serve as an acoustic reflector. A 1100 nm thick aluminum nitride (AlN) piezoelectric layer sandwiched between 2 layers of Mo electrodes (150 nm and 170 nm thick, respectively) forms the acoustic generating part of the transducer. Finally, 200 nm thick AlN and 1000 nm thick SiO_2 were used as passivation layers on the surface to improve device reliability. The transducer was diced into a die of 1 mm × 1 mm and wire bonded to the evaluation board (EVB) for the electric connection, as shown in Fig. 2. The microscope image of the transducer shows the pentagonal resonant area of 0.01 mm^2 in the center of the device. The resonance frequency of the transducer was analyzed by a network analyzer (E5061B, Keysight, USA).

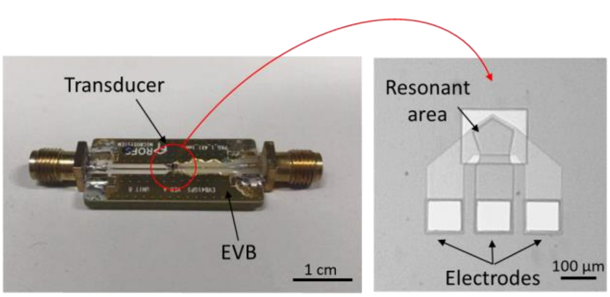

Figure 2. Picture of the microparticle manipulation system. Enlarged view is the microscope image of the gigahertz transducer with a pentagonal resonant area.

B. Particle manipulation system

The generation of the acoustic streaming was controlled by a RF (radio frequency) power supply. A sinusoidal gigahertz signal from a signal generator (SSG-6000RC, Mini-Circuits, USA) was amplified by a power amplifier (ZHL-15W-422+, Mini-Circuits, USA), and applied to the transducer. The transducer and the EVB were immersed in a water tank (14 cm× 11 cm× 11 cm) for particle manipulation. The electrodes of the transducer and the signal line on the EVB were covered with epoxy glue for electrical insulation in water. The distance between the transducer to the water surface was set to be at least 5 cm to ensure that the microparticle movement occurred under water. The horizontal position of the transducer in X-Y plane was controlled by a two-dimensional motorized stage (PILine, PI, Germany), which was connected to the EVB via a customized holder. Glass microbeads (Sigma- Aldrich, 425-600 µm in diameter, ~180 µg) were trapped in our acoustofluidic tweezer. The microparticles' movement was recorded by a camera (EOS 600D with an EF 100mm f/2.8L macro lens, Canon, Japan), and the trajectory was analyzed using ImageJ (Fiji 1.52p, NIH, USA).

C. Characterization of the acoustic streaming

The acoustic streaming generated by the transducer was analyzed using particle image velocimetry (PIV). The transducer was immersed in water filled with fluorescent polystyrene microspheres (15 µm diameter, FluoSpheres®, Life technologies, OR, USA). A plane illumination for the fluorescent excitation (~ 0.5 mm thick and ~10 mm high) was generated by a green laser (532 nm, 100 mW, LD-WL206, Changchun New Industries Optoelectronics Tech. Co., China) and a cylindrical lens. The illumination plane passed through the center of the transducer, and the tracer particles' movement was recorded at 20,000 fps with a high-speed camera (Phantom v7.2, Vision Research, NJ, USA) with a macro lens (EF-S 60 mm, Canon) and a long pass filter (OD4-550nm, Edmund Optics, Barrington, NJ, US). Recorded images were processed by ImageJ, and the streamlines were drawn by overlapping the moving tracks of the particles. The fluidic speed was obtained by calculating the tracer particles' speed in MATLAB (MathWorks, USA) and plotted as a pseudo-color image. When observing the fluid distribution around a glass bead levitated by the acoustic streaming flow, the same laser was used for illumination. Hollow glass beads (10 µm diameter, Dantec Dynamics, Denmark) were added to the water, and the streamlines were recorded by the Canon camera.

III. RESULTS AND DISCUSSIONS

A. Acoustic streaming generated by the gigahertz transducer

Fig. 3(a) shows the streamlines generated by the transducer. An upward jet flow perpendicular to the resonant surface is observed. The velocity distribution of the streaming at 0.5 W power is plotted in Fig. 3(b) using the instantaneous Z-direction velocity of each tracked particle at each position, and is shown in the pseudo-color plot. The result shows the maximal streaming velocity exceeds 0.8 m/s at the position close to the surface of the resonator. The streaming velocity decreases gradually along the Z-direction. The relationship

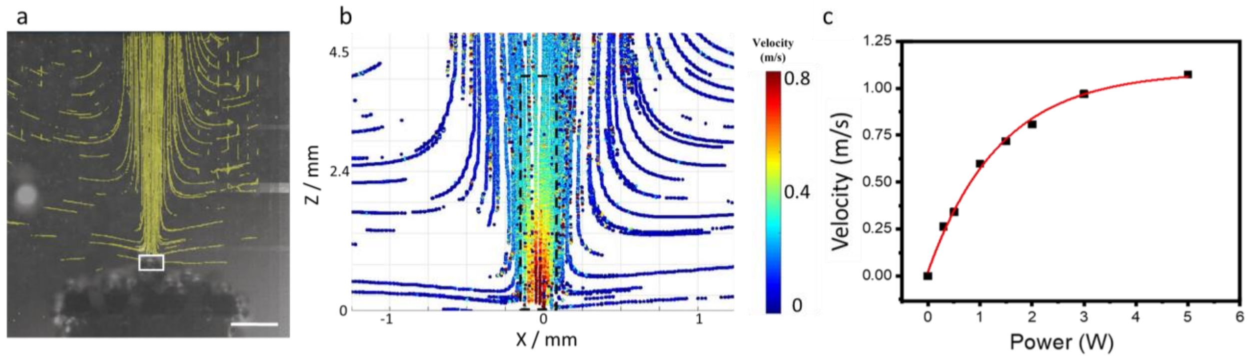

Figure 3. Characterization of the acoustic streaming induced by the gigahertz ultrasonic transducer by PIV. (a) The streamlines (yellow lines) during acoustic streaming. Area marked with the white rectangle corresponds to the center of the transducer. The scale bar is 1 mm. (b) Velocity distribution in the acoustic streaming field. The color indicates the magnitude of the fluidic velocity in Z direction. The transducer is at the position (0, 0). (c) The streaming velocity in the vertical direction (averaged in the black box area shown in b) versus the input RF power.

between the streaming velocity and the input electrical power was also measured and shown in Fig. 3(c). The fluid speed is calculated by averaging the particles' velocity in a 0.265 × 4 mm^2 area near the transducer (marked as the black rectangle in Fig. 3(b)). It reveals that the speed increases nonlinearly as a function of input power, and a maximum speed of over 1 m/s can be realized using this gigahertz transducer.

B. Theoretical analysis of particle trapping in 3D space

The forces acting on the levitated microparticle are shown in the force diagram in Fig. 4(a). Previous publication has confirmed that at the gigahertz frequency, the power of the acoustic wave attenuates to almost zero within hundreds of micrometers in water [33]. In this study, the distance between the manipulated particle and the transducer is over one centimeter, the particle is only affected by the hydrodynamic force but without the influence of the acoustic radiation force. In the vertical direction, the acoustic streaming generated by the transducer provides an upward force to the bead (F_Z). When this force overcomes the gravitational pull on the bead (F_G), the bead levitates. According to the velocity distribution shown in Fig. 3(b), a higher position in Z-direction corresponds to a lower fluid velocity, which corresponds to a smaller lift force for the particle. Thus, the final stable position for the particle is where the lift force generated by the streaming (F_Z) and the buoyancy of the particle (F_B) balance with the particle's gravity (F_G). According to our calculation, the gravitational force on the particle is ~1.8 µN, and its buoyance in water is ~0.6 µN. Thus, the upward hydrodynamic force exerted on the particle at its balance position is ~1.2 µN.

In the horizontal direction, there is also a force balance on the particle to confine it. The flow distribution recorded around the trapped particle is shown in Fig. 4(b), and most streamlines at the center with a width of ~1 mm are vertical. However, due to the low-pressure zone generated by this high-speed fluid motion in the center, liquid on the outer sides of the area is forced to move inwards, which results in oblique flow from the surrounding fluid. As illustrated in Fig. 4(a), fluid on the left moves towards the upper right, thus providing a horizontal force component (F_X). Similarly, fluid on the right moves towards the upper left and provides an opposite force (F_{-X}). Therefore, the particle is centered and also trapped along the horizontal direction.

C. Position control in the vertical direction

The experimental result of the particle trapping can be seen in Fig. 5 (see also Supplementary Video). When certain power is applied to the system, the particle is lifted to the equilibrium position and stably trapped at the position. We observed that the particle can be stably trapped for at least 30 minutes when there is no external fluidic disturbance.

Since the upward fluid velocity can be tuned by using different input powers (Fig. 3(c)), the vertical fluid force distribution can also be adjusted in the same way. When increasing the power, the force provided by the streaming flow increases, thus the particle exhibits a net upward force. With this feature of the system, dynamic position control of the particle in the vertical direction can be achieved.

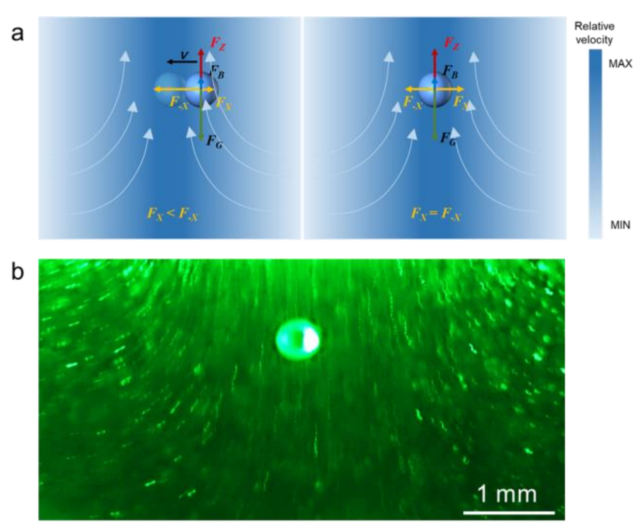

Figure 4. (a) Force diagram of the microparticle at different horizontal positions. Light-blue arrows indicate the fluid flow direction. Fluid velocity variation along X-axis is illustrated by background color variation. The off-center particle (as shown in the left picture) experiences a net horizontal force pointing towards the center where the forces balance (as shown in the right picture). (b) Recorded streamlines around the levitated particle.

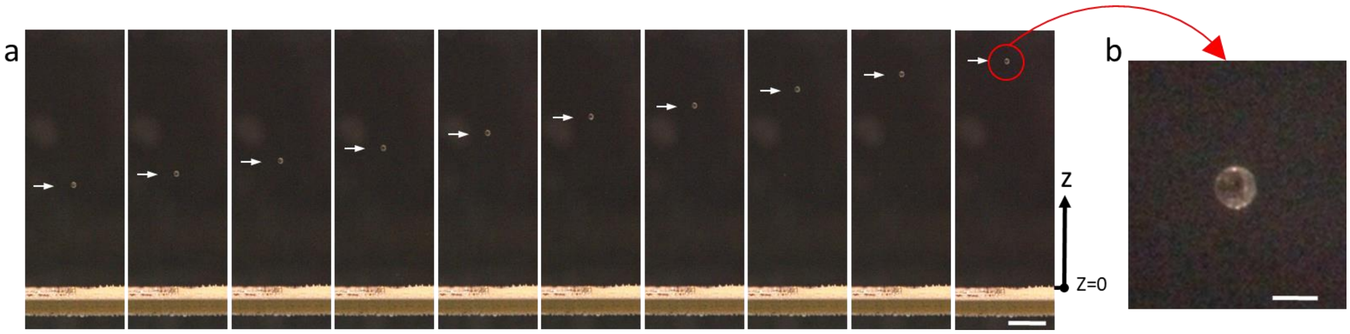

Figure 5. Control of the particle position in the Z direction by tuning the applied power. (a) From left to right: input power increases from 0.4 W (25.95dbm) to 0.7 W (28.45 dBm) with a step of 0.25 dB. White arrows indicate the position of the particle in each frame. Scale bar is 4 mm. (b) Enlarged view of the trapped glass microparticle. Scale bar is 500µm.

Fig. 5 shows the steady-state position of the particle at several different applied electric powers ranging from 0.4 W to 0.7 W. With the increase of the applied power, the distance between particle and the transducer also increases, and the particle is still under control even when the distance exceeds 25 mm (see also Supplementary Video). The position change of the particle rapidly follows the change of the power, and the new location can be stably reached in ~0.5 s. The distance between particle and the transducer under different applied power is plotted in Fig. 6. The Z-position of the microparticle can be linearly controlled by the applied power, and shows good repeatability in both +Z and -Z moving directions. Since the levitation force exerted on the particle balances the gravity of the particle, the trapping position and the stability will be influenced by the size and density of the particle, as well as the fluid viscosity. The detailed relationships between these parameters and the manipulation result will be investigated in future.

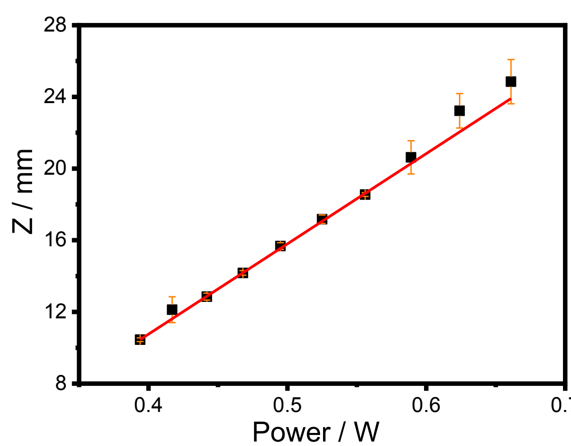

Figure 6. Relationship between the trapping height of the microparticle and the applied electric power. Error bars represent standard deviations.

D. *Dynamic position control in the horizontal direction*

According to the theoretical analysis, the horizontal pressure pushes the particle towards the streaming center. Thus, when the horizontal position of the jet flow moves, the particle will leave the streaming center due to inertia, and the horizontal fluid pressure will push it back towards the balanced position. Fig. 7(a) and 7(b) shows the experiments for dynamic particle position control in the horizontal direction by moving the position of the transducer. The transducer is moved from right to left, and the trace of the particle is observed from the side and the top view. The results show a reliable particle transportation along the X-direction (see Supplementary Video).

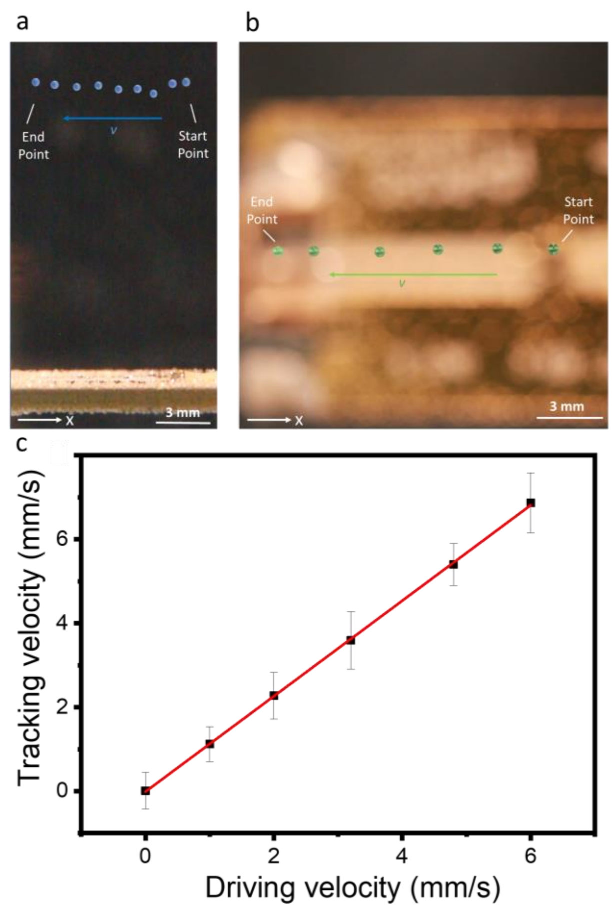

Figure 7. Control of the horizontal position of the microparticle by moving the fluidic tweezer. (a) Overlapped image of the side view of moving a particle at ~0.1 mm/s; (b) Overlapped image of the top view of moving a particle at ~0.3 mm/s. Arrows show the translational direction of the particle. (c) Tracking velocity of the particle versus the driving velocity of the motorized stage. Error bars represent standard deviations.

These two experiments are carried out by moving the transducer slowly, and it is observed that the initial acceleration at the starting point is reflected in a small position instability of the particle. If the driving velocity of the transducer is large, *i.e.* the acceleration is large, then the particle will no longer follow the movement and escape from the trap. In order to study the following capability of the system under high driving speed, motion of the particle is recorded under different driving velocity, and the tracking velocity of the particle is shown in Fig. 7(c). The results show that the system is still stable under a high moving velocity of up to 6 mm/s. Higher speeds result in the loss of the particle from the trap.

E. 2D in-plane position control following a complex trajectory

The manipulation of the microparticle in a 2D plane to follow a designed trajectory is also achieved with the system. A 10 mm× 10 mm square-shaped route is designed and input to the controller of the stage, and the moving speed is set to 0.4 mm/s. The trace of the particle is observed from the top view, and the real particle position during experiment is extracted and displayed as an image series (see Fig.8 and Supplementary Video). The maximum deviation between the particle center to the intended position is ~ 0.2 mm, indicating an excellent positional control. With this result, we believe that complex trajectories in plane can be realized by the system. Together with the position control of the particle in the Z-direction by tuning the power, rapid and stable 3D micro-object manipulation at and over a relatively large distance can be achieved by the acoustofluidic tweezers. Accompanied by other unique features of the gigahertz transducer, such as small volume, low cost, and batch manufacturing, the reported approach can lead to a miniaturized integrated system for micro-robot actuation and untethered micro-manipulation.

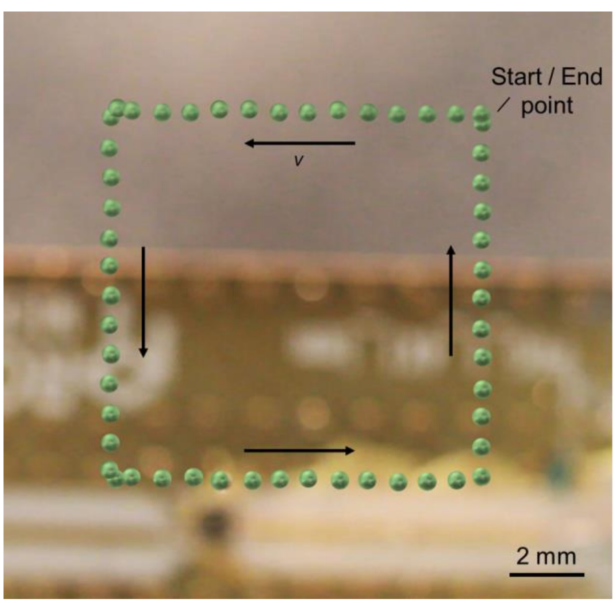

Figure 8. Control of the in-plane position of a microparticle following a square trajectory. The overlapped image shows the moving trajectory of the particle, and the arrows indicate the moving direction. The trasnlational velocity is 0.4 mm/s.

IV. Conclusions

In this paper, we reported a novel manipulation method for microscale (~500 µm) particles to move centimeter distances in liquid environments. Our experimental results show stable particle trapping and rapid particle transportation in 3D. Complex trajectories of a particle is realized by the system with a maximal tracking speed of ~6 mm/s and an accuracy of ~0.2 mm. As the manipulation distance is far from the transducer (larger than 20 times of the particle diameter) and gigahertz ultrasound attenuates very rapidly in water, the acoustic radiation force plays no role in the particle trapping. The method only relies on the hydrodynamic force, which is not restricted by the particle's material property. The method is wireless and permits manipulation without contact to a solid part. Therefore, it holds great potential for the manipulation of fragile, soft and biological materials. Further researches will study the particle manipulation under different fluid viscosity, and the particle size and density. An analytical model of the hydrodynamics will be built to provide a deeper understanding of the trapping mechanism, and shed light to the applications such as multi-particle 3D robotic manipulation.

References

[1] B. L. Walle, M. Gauthier, and N. Chaillet, "Submerged freeze gripper to manipulate micro-objects," in *2006 IEEE/RSJ International Conference on Intelligent Robots and Systems*, 2006, pp. 784-789: IEEE.

[2] K. E. McCloskey, J. J. Chalmers, and M. Zborowski, "Magnetic cell separation: characterization of magnetophoretic mobility," *Analytical chemistry,* vol. 75, no. 24, pp. 6868-6874, 2003.

[3] R. Pethig, "Dielectrophoresis: Status of the theory, technology, and applications," *Biomicrofluidics,* vol. 4, no. 2, p. 022811, 2010.

[4] A. Ashkin, "Acceleration and trapping of particles by radiation pressure," *Physical review letters,* vol. 24, no. 4, p. 156, 1970.

[5] A. Ashkin, J. M. Dziedzic, J. Bjorkholm, and S. Chu, "Observation of a single-beam gradient force optical trap for dielectric particles," *Optics letters,* vol. 11, no. 5, pp. 288-290, 1986.

[6] D. McGloin, "Optical tweezers: 20 years on," *Philosophical Transactions of the Royal Society A: Mathematical, Physical and Engineering Sciences,* vol. 364, no. 1849, pp. 3521-3537, 2006.

[7] D. G. Grier, "A revolution in optical manipulation," *Nature,* vol. 424, no. 6950, p. 810, 2003.

[8] M. D. Wang, H. Yin, R. Landick, J. Gelles, and S. M. Block, "Stretching DNA with optical tweezers," *Biophysical journal,* vol. 72, no. 3, pp. 1335-1346, 1997.

[9] T. Čižmár, L. D. Romero, K. Dholakia, and D. Andrews, "Multiple optical trapping and binding: new routes to self-assembly," *Journal of Physics B: Atomic, Molecular and Optical Physics,* vol. 43, no. 10, p. 102001, 2010.

[10] G. Sinclair, P. Jordan, J. Courtial, M. Padgett, J. Cooper, and Z. J. Laczik, "Assembly of 3-dimensional structures using programmable holographic optical tweezers," *Optics Express,* vol. 12, no. 22, pp. 5475-5480, 2004.

[11] A. Marzo and B. W. Drinkwater, "Holographic acoustic tweezers," *Proceedings of the National Academy of Sciences,* vol. 116, no. 1, pp. 84-89, 2019.

[12] M. A. Andrade, F. Buiochi, and J. C. Adamowski, "Finite element analysis and optimization of a single-axis acoustic levitator," *IEEE transactions on ultrasonics, ferroelectrics, and frequency control,* vol. 57, no. 2, pp. 469-479, 2010.

[13] J. Shi, D. Ahmed, X. Mao, S.-C. S. Lin, A. Lawit, and T. J. Huang, "Acoustic tweezers: patterning cells and microparticles using standing surface acoustic waves (SSAW)," *Lab on a Chip,* vol. 9, no. 20, pp. 2890-2895, 2009.

[14] R. Whymark, "Acoustic field positioning for containerless processing," *Ultrasonics,* vol. 13, no. 6, pp. 251-261, 1975.

[15] D. Foresti and D. Poulikakos, "Acoustophoretic contactless elevation, orbital transport and spinning of matter in air," *Physical review letters,* vol. 112, no. 2, p. 024301, 2014.
[16] A. Marzo, S. A. Seah, B. W. Drinkwater, D. R. Sahoo, B. Long, and S. Subramanian, "Holographic acoustic elements for manipulation of levitated objects," *Nature communications,* vol. 6, p. 8661, 2015.
[17] M. Prisbrey and B. Raeymaekers, "Ultrasound noncontact particle manipulation of three-dimensional dynamic user-specified patterns of particles in air," *Physical Review Applied,* vol. 10, no. 3, p. 034066, 2018.
[18] A. Bernassau, C. Courtney, J. Beeley, B. Drinkwater, and D. Cumming, "Interactive manipulation of microparticles in an octagonal sonotweezer," *Applied Physics Letters,* vol. 102, no. 16, p. 164101, 2013.
[19] P. Glynne-Jones, R. J. Boltryk, N. R. Harris, A. W. Cranny, and M. Hill, "Mode-switching: A new technique for electronically varying the agglomeration position in an acoustic particle manipulator," *Ultrasonics,* vol. 50, no. 1, pp. 68-75, 2010.
[20] F. Guo *et al.*, "Three-dimensional manipulation of single cells using surface acoustic waves," *Proceedings of the National Academy of Sciences,* vol. 113, no. 6, pp. 1522-1527, 2016.
[21] X. Ding *et al.*, "On-chip manipulation of single microparticles, cells, and organisms using surface acoustic waves," *Proceedings of the National Academy of Sciences,* vol. 109, no. 28, pp. 11105-11109, 2012.
[22] K. Melde, A. G. Mark, T. Qiu, and P. Fischer, "Holograms for acoustics," *Nature,* vol. 537, no. 7621, p. 518, 2016.
[23] B. R. Lutz, J. Chen, and D. T. Schwartz, "Hydrodynamic tweezers: 1. Noncontact trapping of single cells using steady streaming microeddies," *Analytical chemistry,* vol. 78, no. 15, pp. 5429-5435, 2006.
[24] V. H. Lieu, T. A. House, and D. T. Schwartz, "Hydrodynamic tweezers: Impact of design geometry on flow and microparticle trapping," *Analytical chemistry,* vol. 84, no. 4, pp. 1963-1968, 2012.
[25] D. Ahmed *et al.*, "Selectively manipulable acoustic-powered microswimmers," *Scientific reports,* vol. 5, p. 9744, 2015.
[26] N. Bertin *et al.*, "Propulsion of bubble-based acoustic microswimmers," *Physical Review Applied,* vol. 4, no. 6, p. 064012, 2015.
[27] W. Cui, M. He, Y. Yang, H. Zhang, W. Pang, and X. Duan, "Hypersonic‐Induced 3D Hydrodynamic Tweezers for Versatile Manipulations of Micro/Nanoscale Objects," *Particle & Particle Systems Characterization,* vol. 35, no. 8, p. 1800068, 2018.
[28] T. Qiu, S. Palagi, A. Mark, K. Melde, F. Adams, and P. Fischer, "Wireless actuation with functional acoustic surfaces," *Applied Physics Letters,* vol. 109, no. 19, p. 191602, 2016.
[29] T. Qiu *et al.*, "Wireless Acoustic-Surface Actuators for Miniaturized Endoscopes," *ACS applied materials & interfaces,* vol. 9, no. 49, pp. 42536-42543, 2017.
[30] Z. Ye and M. Sitti, "Dynamic trapping and two-dimensional transport of swimming microorganisms using a rotating magnetic microrobot," *Lab on a Chip,* vol. 14, no. 13, pp. 2177-2182, 2014.
[31] T. Petit, L. Zhang, K. E. Peyer, B. E. Kratochvil, and B. J. Nelson, "Selective trapping and manipulation of microscale objects using mobile microvortices," *Nano letters,* vol. 12, no. 1, pp. 156-160, 2011.
[32] Q. Zhou, T. Petit, H. Choi, B. J. Nelson, and L. Zhang, "Dumbbell fluidic tweezers for dynamical trapping and selective transport of microobjects," *Advanced Functional Materials,* vol. 27, no. 1, p. 1604571, 2017.
[33] X. Guo, H. Zhang, Y. Wang, W. Pang, and X. Duan, "Programmable multi-DNA release from multilayered polyelectrolytes using gigahertz nano-electromechanical resonator," *J Nanobiotechnology,* vol. 17, no. 1, p. 86, Aug 6 2019.